International Journal of Thin Films Science and Technology

http://dx.doi.org/10.18576/ijtfst/110204

Some Optical Investigations Thin Films of $Ga_{80-x}Se_xTe_{20}$ (where x=15% and 20%) Chalcogenide glass

Khadijah M. AL. Mokhtar

Physics Department, College of Science, Taibah University, Medina, Kingdom of Saudi Arabia

Received: 20 Jul. 2020, Revised: 10 Nov. 2020, Accepted: 15 Nov. 2020

Published online: 1 May 2022

Abstract: Thin films of $Ga_{80-x}Se_xTe_{20}$. Chalcogenide glass with thickness (x = 15 and 20) were deposited on a chemically cleaned glass surface by thermal evaporation technique. The absorption spectra of the prepared samples were studied using spectrophotometers in the wavelength range 200-2500 nm. The optical parameters like absorption coefficient (α), extinction coefficient (k) and the optical bandgap (Eg) is calculated for the system. $Ga_{80-x}Se_xTe_{20}$.glassy the optical energy gap, is the result of both direct and indirect permissible transformations. E_g decreased from 2.237eV to 2.137eV when the transition is direct and from 1.114569 to1.05984 ev for indirect transition by increasing Se content. While the band tail width energy give the opposite trends For all samples, the reduction coefficient (k) is lowered by the wavelength (λ). The absorption coefficient (α) was found to increase with the incident photon energy (hν) for both concentrations. Also, it is noted that both k and α increases with increasing Se concentration in a-$Ga_{80-x}Se_xTe_{20}$.glassy system. The reduction in optical band gap with increase in Se concentration may be attributed to an increase in the amount of disorder in the materials and increase in the density of defect states. Other optical parameters have been evaluated such as Dispersion energy, "E_d", single oscillator energy, "E_0", and static refractive index, "n", have been calculated According to the mode Wemple–DiDomenico model. Also, other parameters have been calculated such dielectric constant at infinite wavelength ε_∞, lattice dielectric constant ε_l, concentration of the charge carriers per effective mass N/m*, N concentration of the charge carriers. Due to the large absorption coefficient and component reliance on absorption, these materials may be appropriate for optical devices.

Keywords: chalcogenide glasses, optical properties, thin films , Dielectric Constants , band gap

1 Introduction

Recently, the research of chalcogenide glasses has aroused great interest from the point of view of basic physics as well as of device technology. They are suitable for optical components, optical discs, functional components in integrated optical systems, infrared fibers with high flexibility and chemical durability [1-6], etc. It has been observed that the compositional changes of glassy chalcogenide semiconductors have a significant impact on the band gap and optical properties [7]. It is well known that the optical constants (absorption coefficient (α), extinction coefficient (k) in addition to band gap (Eg) are the most important parameter in amorphous semiconductor films. Using the optical properties of the material, its optical constants can be determined. Therefore, the measurement accuracy of optical constants is very important. The purpose of this article is to study the effect of selenium doping on the optical properties of Ga-Te matrix.. Light absorption spectrum of the film of $Ga_{80-x}Se_x$ Te_{20} (x = 15 and 20) are measured in the wavelength range 200-2500 nm, by double beam UV-VIS spectrophotometer. Optical parameters like absorption coefficient (α), k the band tail width E_e, extinction coefficient (k) and optical band gap (E_g) have been calculated for $Ga_{80-x}Se_x$ Te_{20} glassy system.

2 Experimental Techniques

Bulk amorphous of $Ga_{80-x}Se_xTe_{20}$ (where x = 15 and 20 at %) chalcogenide glass were Prepared using conventional melt quenching technology [11]. The high purity (99.9999% purity) materials of Ga, Se and Te are weighed according to atomic percentage and sealed in a quartz ampoule with a vacuum of 10^{-5} Torr. The sample was heated and melted in a rocking furnace, and the temperature was gradually increased at a rate of 4 K/min for 12 hours to 1273 K. During the heating process, the ampoule is often

*Corresponding author E-mail: khmadina@yahoo.com

shaken by rotating the ceramic rod, and then the amorphous substance is stuffed into the furnace to obtain a melt with uniform composition. The molten sample is then quickly quenched in ice-cooled water. Take out the quenched sample by destroying the ampoule to obtain the bulk material the thin films of $Ga_{80-x}Se_xTe_{20}$ were prepared from their bulk compositions in homogeneous form. Using an Edwards E306 coating device operating at 10-5 Torr, the bulk glass of the composition was heated to a chemically cleaned glass substrate by thermal evaporation. Direct thermal evaporation is carried out from a small quartz crucible, which uses a conical basket of tungsten wire as the filament for heating. The evaporation is initiated by passing a low current in the filament for a time sufficient to heat the material. The current is gradually increased carefully, and as the material melts in the crucible, the current will increase rapidly to avoid decomposition of the sample. The film is deposited on different substrates. The mechanical rotation of the glass substrate holder helps to deposit uniform thin films at a high deposition rate of 10 nm/s. film thicknesses, in the range of 516 and 1028 nm, were measured using a quartz crystal thickness monitor (FTMS, Edwards, UK) [8]. The earthed face of the crystal monitor was facing the source and was placed at the same height as the substrate. The margin of error in the obtained thickness was 0.05%.

The optical absorption and transmission data were obtained using a computerized UV- 2101 double-beam spectrophotometer in the wavelength range of (500-2500 nm) throughout the experiment.

3 Results and Discussion

3.1 Optical Properties

3.1.1. Absorption Coefficient (α) and Optical Band Gap (E_g)

The absorption coefficient (α) of the film was calculated using equation **(1).**

$$\alpha = OD/t, \qquad (1)$$

where OD is the optical density measured on a layer of a given thickness (t). A plot of absorption coefficient (α) as a function of photon energy (hυ) As shown in Figure 1, it has been observed that absorption coefficient (α) increases with increase in photon energy (hυ) as well as Se concentration, for both $Ga_{80-x}Se_xTe_{20}$ film samples.

Because of the value of absorption coefficient, α, in the absorption region, two important parameters can be evaluated, namely, tail width, Ee, and the optical energy gap, E_g. In the region, where 1 cm^{-1}< α <$\mathbf{10^4}$ cm^{-1}, Absorption occurs between the tail of the valence band and the extended state of conduction. The absorption coefficient is given by the empirical relationship and depends on the photon energy [9].

$$\boldsymbol{ln\,\alpha = lnB + \frac{h\upsilon}{E_e}} \longrightarrow \qquad (2)$$

where B is a constant and E_e tail width corresponds to the tail width of the local state at the edge of the belt into the energy gap and generally Ee represents the degree of disorder in an amorphous semiconductor [10]. The value of E_e is determined from the reciprocal of the slope of the relation between ln α and hν as given in Figure 2, for $Ga_{80-x}Se_xTe_{20}$ films as representative examples.

For α > 10^4 cm^{-1}, Absorption occurs between the valence state and the conduction band extension state, and has the form mentioned by Davis and Mott [11,12].

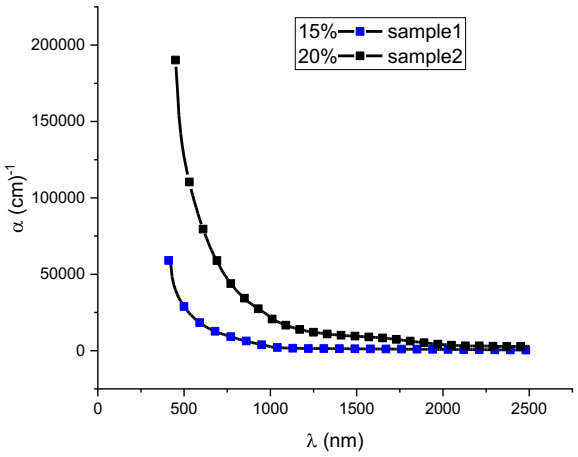

Fig. (1): Plot of α vs hυ for $Ga_{80-x}Se_x$ Te_{20}(x=15 and 20) thin film.

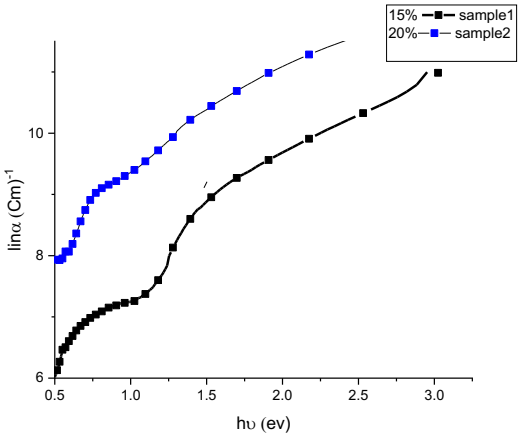

Fig. (2): Plot of ln α vs hυ for $Ga_{80-x}Se_x$ Te_{20}(x=15 and 20) thin film.

The absorption coefficient (α) is obtained directly from the absorbance relative to the wavelength curve using the following relationship

$$(\alpha h\upsilon) = A(h\upsilon - E_g)^r \qquad \textbf{(3)}$$

υ is the photo frequency; h is the Planck's constant. A is an edge width parameter representing the quality of the film, calculated from the linear part of the relationship, Eg is the optical band gap of the material, and r is an index that depends on the type of band transition involved;r= ½ or 3/2 for the allowed inter band transition and forbidden direct inter band transition respectively , but r = 2, 3 allowes indirect inter band transition and forbidden indirect inter band transitions respectively. The intercept of the linear extrapolated fit to the experimental data of the relation $(\alpha h\upsilon)^2$ verses incident photon energy hυ gives the value of the direct optical band gap energy, while the extrapolation of the linear part of the plot $(\alpha h\nu)^{1/2}$ verses incident photon energy hν gives the value of the indirect optical band gap energy of the investigated film.

The variation of $(\alpha h\nu)^{1/2}$ with (hυ) for a- $Ga_{80-x}Se_x$ Te_{20}(x=15 and 20) thin film are shown in Figure3.

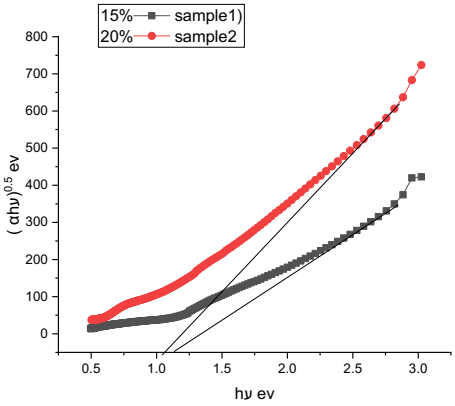

Fig. (3): Plot of $(\alpha h\upsilon)^{1/2}$ vs hυ for $Ga_{80-x}Se_x$ Te_{20}(x=15 and 20) indirect transition in two sample thin films.

The observed indirect transitions with assisted photon are listed in Table1 for two thin films.

Table.1: Indirect band gap energy, photon assisted energy for two thin films.

Sample no	Compounds	Indirect band gap energy ev	photon Energy $\mathbf{E_{ph}(ev)}$ **ev**
1	$Ga_{80-x}Se_{15}$ Te_{20}	1.114569	37
2	$Ga_{80-x}Se_{20}$ Te_{20}	1.05984	110

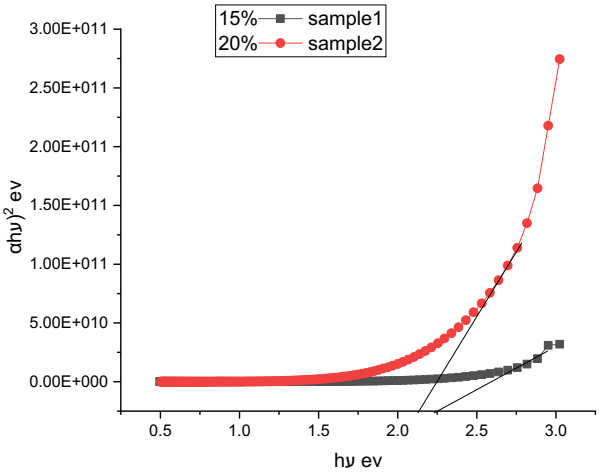

Fig. (4): *Variation of* $(\alpha h\upsilon)^2$ vs incident photon energy hυ for $Ga_{80-x}Se_x$ Te_{20}(x=15 and 20) direct transition in two sample thin films.

Table 2: Direct optical band gap and band tail width energies for $Ga_{80-x}Se_x$ Te_{20} thin films.

Sample no	*Compounds*	Direct band gap energy(eV)	Band tail width E_e eV
1	*$Ga_{80-x}Se_{15}$ Te_{20}*	*2.237*	*0.398*
2	*$Ga_{80-x}Se_{20}$ Te_{20}*	*2.137*	*0.543*

The values of indirect and direct band gap (E_g) have been calculated by taking the intercept on the x-axis. The calculated values of direct band gap E_g for all glassy samples of a- **$Ga_{80-x}Se_x$ Te_{20}** are given in Table2. It is evident from the Tables 1,and 2 that the values of optical band gap (E_g) decrease with increasing Se concentration. A decrease in the optical band gap Eg indicates an increase in the density of defect states. The reduction of the optical band gap can also be discussed on the basis of the state model density proposed by Mott and Davis [13]. It is found that the band gap energy is inversely proportional to the Urbach energy. Chalcogenide films always contain a high concentration of unsaturated bonds or defects. These defects are the cause of the local state in the amorphous band gap. The decrease in Eg and the increase in the density of defect states may also be related to the electronegativity of the involved elements [14]. he valence band in chalcogenide glass is formed by the loan pair orbitals contributed by chalcogen atoms [15]. The energy of these loan-pair electrons adjacent to the electronegative atoms will be higher than the energy of the electronegative atoms. Therefore, adding a positive electric element to a negative electric element can increase the energy of the

lone pair state, which further causes the valence band within the band gap to widen. The electronegativity of Se and Ga are 2.1 and 1.8 1respectively. Since Ga has lower electronegativity than Se, the substitution of Ga for Se It may increase the energy of the lone pair state, which may further cause the expansion of the valence band. This leads to band tailing and therefore the band gap shrinks. Therefore, Eg decreases with Se content. In addition, Urbach energy or tail width, E_e, has been used to characterize the degree of disorder in the low crystalline or partially crystalline materials as well as amorphous materials. It is believed that the tail width associated with the valence and conduction bands originates from electronic transitions between local states, where the density of these local states is exponentially related to the incident photon energy.

3.1.2 Optical Refractive Index (n).

The refractive index is the basic optical parameter of the material, because its value can well indicate the dispersion of light. It is also useful in developing nonlinear phenomena. Therefore, the study of this parameter is very important. The transmittance (T) and reflectance values (R) are corrected using software programs, and further used to calculate the refractive index [16,17]. Murmann's exact equations are used and minimize both of $|\Delta R|^2$ and $|\Delta T|^2$ simultaneously, [17,18]:

$$(\Delta R)^2 = (R_{exp} - R_{cal})^3 \quad \text{and} \quad (\Delta T)^2 = (T_{exp} - T_{cal})^2 \qquad \textbf{(4)}$$

where, R_{exp}, R_{cal} are experimental and calculated values of reflection and T_{exp} and, T_{cal} correspond to experimental and computed values of transmission. The refractive index of the $Ga_{80-x}Se_xTe_{20}$ films is computed as follows [15,16,18]:

$$T = 4n / (n - 1)^2 \quad \text{and} \quad R = (n - 1)^2 / (n+1)^2 \qquad \textbf{(5)}$$

with value of both the high extinction coefficient, k and the absorption, the reflectance values 'R' must be corrected as was assumed by Kramers–Kronig relation [15,16,18]:

$$R = [(n - 1)^2 + k^2] / [(n - 1)^2 + k^2] \qquad \textbf{(6)}$$

Therefore, using this equation, Calculate the refractive index spectrum n and express it as a function of photon wavelength in Figure 5. It can be seen that at lower wavelength values, that is, in the strong absorption region of the electromagnetic spectrum, the refractive index values show abnormal (or resonant) dispersion behavior.. In the strong absorption region ($\lambda \ll$ 800 nm), the incident photon frequency is almost equal to the plasma frequency, which is attributed to the higher refractive index in this region. After $\lambda \geq 700$ nm, the refractive index drops sharply with the wavelength and shows obvious normal dispersion. At higher wavelengths (lower photon energy), the value of n becomes almost constant. In addition, it can be clearly seen from the figure that as the Se content increases, the refractive index value increases (for the entire wavelength region), that is. the refractive index values depend upon the stoichiometry of Ga_{80-x} Se_xTe_{20}. glassy matrix. Therefore, these results may be due to the changes in the structure of the film sample and due to also the bonding arrangement [19,20]. It is worth to mention that Ga_{80-x} Se_xTe_{20} films and some similar materials, with high refractive index values, are of great importance, this increase in refractive index values attributes to the enlarged polarizability values connected with the Se atom [21], which has a larger size than Ga. In addition, in the low frequency region ($\lambda \geq 1700$ nm), the refractive index value slowly increases, and the Se content increases from 15% to 20%. The refractive index values obtained from the experiment are plotted in Figure 5 and listed in Table 3.

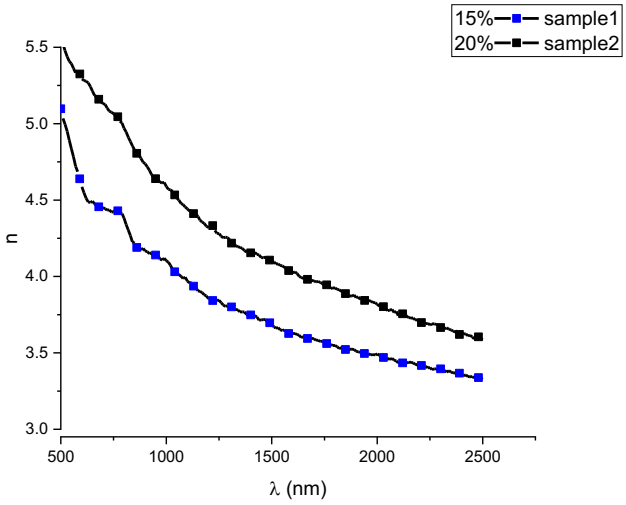

Fig. (5): Variation of refractive index vs wavelength λ (nm) for chalcogenide$Ga_{80-x}Se_x$ Te_{20}(x=15 and 20)thin film where, x = 15 and 20 at. %.

3.1.3 Optical Extinction Coefficient, (k).

The extinction coefficient k describes the propagation and speed of electromagnetic waves in solid materials and films. The k value also describes the damping that occurs or the oscillation amplitude damping of the electric field component of the wave, so it is also called the absorption index. The basic optical parameter (k) can also be derived from the transmission spectrum and the reflection spectrum according to Equation 7. [15,16]:

$$K(\lambda) = \frac{\lambda}{4\pi} lin \left[\frac{(1-R)^2}{2T} + R^2\right] \qquad (7)$$

Where λ is the wavelength of the incident photon, (λ is in nm), and T is the film thickness. The spectral change of the extinction coefficient k with the wavelength of the incident photon is shown in Figure 6.shows the spectral dependence of k for $Ga_{80-x}Se_xTe_{20}$ (x = 15, 20) thin films with wavelength (λ) in thin films samples. t can be clearly seen

from the figure that the k of all samples decreases with the increase of λ. This behavior is due to the decrease in absorption coefficient as λ increases. It can also be seen from Table 3that k increases with Se concentration in thin films.

A decay or damping in the NIR-spectral region of wavelength, at λ ≥ 1400 nm is also noticed. Moreover, the absorption index values, k slightly increases as Se-content increases. Mott, Davis and others have found this similar behavior for many amorphous semiconducting materials [15,16,22 -24].

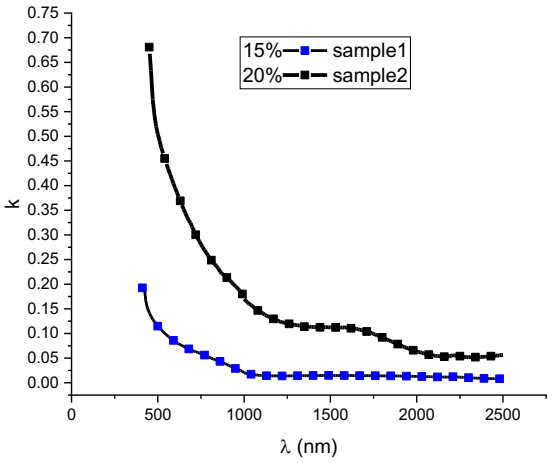

Fig. (6): Plot of extinction (K) vs (λ) for $Ga_{80-x}Se_x$ Te_{20}(x=15 and 20) thin film

3.1.4 Refractive Index Dispersion and Dispersion Energies.

Single Effective Oscillator Model and Wemple and Di-Domenico Parameters.

The variation of the refractive index dispersion of the investigated samples can be understand and analyzed in terms of single effective oscillator model proposed by "Wemple and Di-Domenico" (also called "Single Effective Oscillator Model, SEO-Model"). The model suggests that the refractive index n of the investigation film is simply related to the electronic structure of the film material by equation:

$$(n^2\text{-}1) = E_0E_d/(E_0^2\text{-}(h\upsilon)^2) \quad \textbf{(8)}$$

where, E_0 is the energy of a dispersive oscillator of electronic transport and 'Ed' dispersion energy, which related the average oscillator strength of optical transition [25-28], .As shown Eq (8) , the values of E_0 and E_d can be extracted from graphical representation of Figure 7 illustrates the variation of $(n^2 - 1)^{-1}$ (y-axis) vs $(h\upsilon)^2$ (x-axis) . The intersection point of the line at $(h\upsilon)^2 = 0$ refer to the value of ε_∞ the optical dielectric constant at high frequency. The calculated values of E_0 and E_d, and ε_∞ are given in table3.

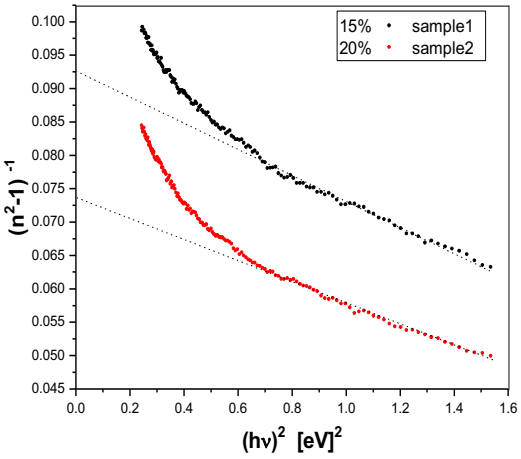

Fig. (7): Plot of (n-1)-1 vs (hυ)2 for Ga80-xSex Te20(x=15 and 20) thin film.

3.2 Dielectric Constants

To gain more understanding of physical properties of the material under investigation, it's appropriate to the more information about the lattice dielectric constant and carrier concentration (N). According to spitzer et al.model, the real component of dielectric constant ε is related to (λ^2) by following relation [29] :

$$n^2 = \varepsilon_l - \left(\frac{e^2}{4\pi^2 c^2 \varepsilon_0}\right) (N/m^*)\,\lambda^2 \qquad (9)$$

where c is the speed of light, e is the elementary charge, ε_0 is the permittivity of free charge, . N/m* is the ratio of free carrier concentration to the effective mass, ε_L is the lattice dielectric constant, the behavior of n^2 with λ^2 is shown in **Figure 8** which satisfy a flat line at high wavelengths. The value of ε_L and N/m^* are given from the intersection of the flat line of λ^2=0 , while N/m^* given from the slope.

The deduced values of both (N/m*) and ε_l are listed in Table 3. The index of refraction increase with increase Se content as well as when the frequency of electromagnetic wave passes through the region of distinctive electron frequency. Also both ε_l and ε_∞ are greater than n , this is may be due to the exitance of the free charge carriers in amorphous film samples of the $Ga_{80-x}Se_x$ Te_{20}(x=15 and 20) thin film are strongly contributing in the polarization process[23] .The charge carrier N can be computed from the ratio (N/m*) and the electron rest mass m^* and m_0 . the increase of charge carrier concentration attributes to the high atomic number of Se as compared to Ga.

Table.3: Values of The absorption coefficient (α), extinction coefficient k, Optical refractive index n., the single -oscillator energy E_0, dispersion energy E_d . dielectric constant at infinite wavelength ε_∞, lattice dielectric constant ε_L, concentration of the charge carriers per effective mass N/m*, N concentration of the charge carriers.

	α(Cm)$^{-1}$	K	n	E_0 ev	$E_d$ev)	ε_∞	ε_L	N/m* (gm^{-1} cm^{-1})	N (cm−3)
$Ga_{80-x}Se_{15}$ Te_{20}	59040	0.19262	5.3337	2.235	24.54	11.98	14.85	$6.14x10^{56}$	$2.484x10^{26}$
$Ga_{80-x}Se_{20}$ Te_{20}	190200	0.68095	5.8968	2.135	28.83	19.504	18.15	$1.6x10^{57}$	$6.82011x10^{26}$

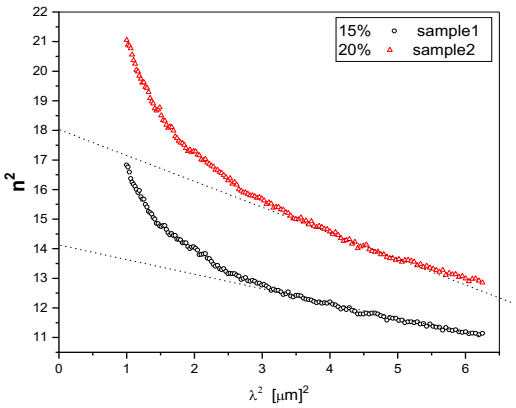

Fig. (8): Plot(n)^2 vs (λ)^2 for $Ga_{80-x}Se_x$ Te_{20}(x=15 and 20) thin film.

4 Conclusions

Thin films of $Ga_{80-x}Se_xTe_{20}$. Thickness chalcogenide glass (516 and 1028 nm) is placed on a chemically cleaned glass surface using thermal evaporation technique.
Absorption coefficient (α) is found to increase linearly with incident photon energy (hν) for both samples. It has further been observed that both k and α increases with increasing Se concentration in a- $Ga_{80-x}Se_x$ Te_{20} glassy system. Itis also observed that optical band gap decreases with increasing Se content. While An inverse relation between optical band gap energy and Band tail width energy was found. The decrease in optical band gap with increase in Se concentration may be due to the increase in the amount of disorder in the materials and increase in the density of defect states. The reduction in bandgap can also be explained by the difference in electronegativity between the elements involved in the formation of the $Ga_{80-x}Se_x$ Te_{20} - glassy system due to the large absorption coefficient. And, depending on the absorption, they may be suitable for optical devices.

Conflict of Interest

All authors declare that there is no conflict of interest regarding the publication of this paper.

References

[1] A. M. Adam et al., Mater. Chem. Phys. 224 (2019) 264–270.

[2] A. Medjouri, D. Abed and Z. Becer, Opto-Electronics Rev. 27 (1) (2019) 1–9.

[3] J. Barták, P. Koštálb, and J. Málek , J. Non-Cryst. Solids., 505 1–8(2019).

[4] A.S. Hassanien and A.A. Akl , J. Non-Cryst. Solids., **428**, 112-120(2015).

[5] Bekir Karasu et al., Journal of Science and Engineering., **6(3)**, 428-457(2019).

[6] P. Petkov et al., Journal of Opto electronics and Advanced Materials., **7(4)**, 1965 – 1969(2007).

[7] A. S. Hassanien and Ishu Sharma, Optik - International Journal for Light and Electron Optics., **200**, 163415(2020).

[8] M.M. El-Nahass, A.A.M. Farag and H.E.A. El-Sayed, Appl. Phys., **A77**, 819-826(2003)

[9] F. Urbach, (1953) Phys. Rev. 92 1324.

[10] J. A. Olley, (1973) Solid State Commun. 13 1437.

[11] J. Tauc , Grigorovici R and Vancu A (1966), Phys. Status Solidi B15 627.

[12] E. A. Davis and N. F. Mott , (1970) Philos. Mag. 22 903.

[13] N.F. Mott and E.A. Davis, Electronics Processes in Non – Crys Mat., Clarendon, Oxford, (1979), 428.

[14] Kh. M. Al Mokhtar and B. O. Alsobhi, New Journal of Glass and Ceramics, (2017) 7, 9199.

[15] A.S. Hassanien and A.A. Akl, Appl. Phys. A. 124 (2018) 752.

[16] A.S. Hassanien and A.A. Akl, J. Alloys. Compd. 648 (2015) 280–290.

[17] S.A. Mahmoud, A.A. Akl and S.M. Al-Shomar, Physica B 404 (2009) 2151– 2158.

[18] O.S. Heavens, "Optical Properties of Thin Solid Films", Dover, New York, (1965).

[19] M.I. Abd-Elrahman et al., Spectrochim. Acta, Part., **A137** 29–32(2015).

[20] M. Kincl and L. Tichy, Chem. Phys., **110**, 322–327(2008).

[21] M. Mohamed and M.A. Abdel-Rahim, Vacuum., **120**, 75–

80(2015).

[22] A.S. Hassanien and I. Sharma, J. Alloys. Compd., **798**,750–763(2019).

[23] A.S. Hassanien, , J. Alloys. Compd., **671**,566–578(2016).

[24] N.F. Mott, E.A. Davis, "Electronic Processes in Non-crystalline Materials", Clarendon Press, Oxford, (1979).

[25] A. S. Hassanien a,b,∗ , IshuSharmac, Optik - International Journal for Light and Electron Optics., **200**, 163415(2020).

[26] S.H. Wemple and M. Di-Domenico, Phys. Rev. **B 3**, 1338–1350(1971).

[27] S.H. Wemple, Phys. Rev., **B 7**, 3767–3776(1973).

[28] Q. Shen and T. Toyoda, J. Appl. Phys., **45 (6B)**, 184–185(2005).

[29] Bezryadina,A.,France, C.,Graham, R.Yang,L.,Carter,S.A.,et al. Appl. phys. lett., **100**, 013508(2012).